Membrane Conformations and Their Relation to Cytotoxicity of Asimicin and Its Analogues†

Hiroko Shimada,‡ John B. Grutzner,§ John F. Kozlowski,‡ and Jerry L. McLaughlin*,‡

Department of Medicinal Chemistry and Molecular Pharmacology, School of Pharmacy and Pharmacal Sciences, and Department of Chemistry, School of Sciences, Purdue University, West Lafayette, Indiana 47907

Received September 22, 1997; Revised Manuscript Received November 10, 1997

ABSTRACT: Certain plant species belonging to the family Annonaceae produce Annonaceous acetogenins, which are a unique class of long-chain fatty acid derivatives with potent cytotoxicity. Putative protein targets of the acetogenins are membrane-associated proteins, including complex I. Asimicin and its analogues constitute a class of Annonaceous acetogenins containing two tetrahydrofuran (THF) rings with hydrocarbon chains tethered to each ring; an α,β-unsaturated γ-lactone ring is terminal to one of the alkyl chains. The compounds examined in this study differ in the length of the alkyl chain between the THF rings and the lactone ring. The positions of both the THF and the lactone rings within liposomal membranes were determined by proton (^{1}H) nuclear magnetic resonance spectroscopy. The depth of membrane penetration of acetogenins, coupled to membrane diffusion, controls the conformation of acetogenins as they diffuse to an active site. Based on ^{1}H intermolecular nuclear Overhauser effects (NOEs), the THF rings of all acetogenins studied reside near the polar interfacial head group region of the DMPC. This was corroborated by ^{1}H two-dimensional NOE spectroscopy and differential scanning calorimetry studies. The ^{1}H difference NOE spectra indicated that the lactone rings of asimicin and parviflorin, the latter of which has two fewer carbons in its alkyl chain, are located below the glycerol backbone in the membrane. In contrast with asimicin and parviflorin, the lactone ring of longimicin B, an asimicin analogue with an alkyl chain four carbons shorter, resides close to the midplane in the membrane. This was corroborated by manganese-induced broadening studies. Since the THF rings are located near the center of the acetogenin molecules and the lactone ring is terminal to a long alkyl chain, these observations indicate that an asimicin-type acetogenin can be in either sickle-shaped or U-shaped conformations, depending on the length of the alkyl chain between the THF rings and the lactone ring. Interestingly, longimicin B does not exhibit significant cytotoxicity, but parviflorin is as cytotoxic as asimicin. The cytotoxicity of the asimicin-type of acetogenins would seem to be strongly related to the membrane conformation. This is the first report elucidating the conformation of Annonaceous acetogenins in membranes.

Annonaceous acetogenins are bioactive secondary plant metabolites found only in several genera of the family Annonaceae (*1*−*5*). Asimicin (**1**) and its analogues (Figure 1) constitute a class of Annonaceous acetogenins containing adjacent bis-tetrahydrofuran (THF)[1] rings flanked by hydroxyl groups on hydrocarbon chains with *threo-trans-threo-trans-threo* configurations from C-15 to C-24. In addition, **1** contains a terminal α,β-unsaturated γ-lactone ring and a 4-hydroxyl. Acetogenins are known to be very potent cytotoxic compounds. Putative protein targets are the reduced nicotinamide adenine dinucleotide (NADH): ubiquinone oxidoreductase in complex I, which is a membrane-bound protein of the mitochondrial electron transport system (*6*, *7*), and the ubiquinone-linked NADH oxidase in the plasma membrane of cancerous cells (*8*). The three compounds (**1**−**3**) studied have similar chemical structures, differing only in the alkyl chain length. However, they exhibit quite different cytotoxicity profiles; **3** shows very little cytotoxicity as opposed to **1** and **2**, which are very cytotoxic (*3*, *4*). For example, the brine shrimp lethality test (BST) used as a bench-top assay whose activity is related to cytotoxicity (*9*) showed LC_{50} values of 3.0×10^{-2}, 9.0×10^{-2}, and 8.0 μg/mL for compounds **1**−**3**, respectively.

Acetogenins are generally lipophilic and are expected to be quantitatively associated with membranes. This suggests that they must gain access to their protein target sites by diffusion within the membrane. The crystal structure of gigantecin, the only natural acetogenin to be characterized

† This work was supported by R01 Grant CA30909 from the National Cancer Institute, National Institutes of Health.

* Author to whom correspondence should be addressed.

‡ Department of Medicinal Chemistry and Molecular Pharmacology, School of Pharmacy and Pharmacal Sciences.

§ Department of Chemistry, School of Sciences.

[1] Abbreviations: CH_2Cl_2, dichloromethane; DMPC, dimyristoylphosphatidylcholine; DOF, decoupler offset; DSC, differential scanning calorimetry; ^{1}H, proton; HPLC, high-performance liquid chromatography; MLV, multilamellar vesicle; NADH, reduced nicotinamide adenine dinucleotide; NMR, nuclear magnetic resonance spectroscopy; NOE, nuclear Overhauser effect; NOESY, two-dimensional NOE spectroscopy; SUV, small unilamellar vesicle; THF, tetrahydrofuran; TLC, thin-layer chromatography; T_m, transition temperature; τ_m, mixing time.

S0006-2960(97)02348-9 CCC: $15.00
Published on Web 01/06/1998

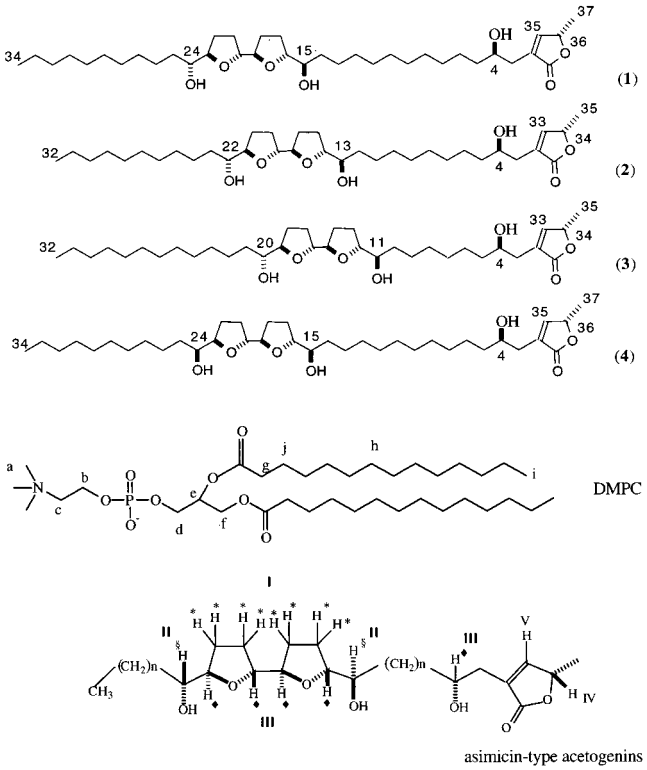

FIGURE 1: Structures of the acetogenins studied, (**1**) asimicin, (**2**) parviflorin, (**3**) longimicin B, and (**4**) bullatacin, and chemical group assignments of DMPC and asimicin-type acetogenins (**1**−**3**). ^{1}H chemical shift assignments are shown in Table S 2. I: protons labeled with *. II: protons labeled with §. III: protons labeled with ◆.

by X-ray crystallography, indicates that it occurs in an extended conformation (*10*). However, membrane and not crystal energetics determines the conformation of a lipophilic compound acting at a membrane receptor in the lipid bilayer (*11*−*13*). The efficiency of binding for low concentrations of such a drug to an intrabilayer receptor site could be increased by limiting it to a specific region of the membrane, which reduces the degrees of freedom of the drug.

For this work, it was hypothesized that acetogenins partition into lipid membranes and adopt a favorable conformation within the membrane. The length of the chain between the two ring systems of an acetogenin may regulate its membrane conformation and, thus, determine the cytotoxicity of the acetogenin. Despite a number of studies on their structure−activity relationships in exerting biological effects (*14*−*18*), little is known about how acetogenins interact with the membrane bilayers.

Several spectroscopic techniques, including nuclear magnetic resonance (NMR) spectroscopy, have been applied to investigate drug−membrane interactions (*19*−*21*). Most of the solution proton (^{1}H) NMR studies of drug−membrane interactions utilize detergent micelles or organic solvents instead of bilayer membranes (*22*, *23*). However, the packing of phospholipids in micelles is remarkably different from that in a bilayer (*24*). Determining the location and the conformation of acetogenins in membranes seems to be necessary to understand their role as potent cytotoxic compounds.

In this study, small unilamellar vesicles (SUVs) made from dimyristoylphosphatidylcholine (DMPC) were used for ^{1}H NMR measurements, and multilamellar vesicles (MLVs) were used for differential scanning calorimetry (DSC) studies. The membrane conformations of acetogenins were elucidated by determining the locations of the THF rings and the lactone ring of the acetogenin in the artificial membrane using ^{1}H NMR spectroscopy. DSC studies on DMPC with acetogenin dispersions showed that the acetogenins strongly interact at the hydrocarbon core/water interface of DMPC (*25*).

The results of ^{1}H NMR studies indicate that all acetogenins studied have strong interactions between the protons of the THF rings of the acetogenins and those of the glycerol backbone of DMPC, as suggested by the DSC studies. The NMR studies also indicate that the conformation of an asimicin-type acetogenin depends on the length of the alkyl chain between the two ring systems in the compound. Both **1** and **2**, with 13- and 11-carbon alkyl chains, respectively, between the two ring systems, are sickle shaped in the membrane, i.e., the THF rings of both compounds are located very close to the head groups of DMPC, and the lactone rings of these compounds are situated in the midchain area between the head groups and the terminal methyl groups of DMPC. On the contrary, **3** with a nine-carbon alkyl chain between the two ring systems, is U-shaped in the membrane, i.e., the THF rings of **3** are located close to the head groups of DMPC, as in **1** and **2**, but the lactone ring of **3** is located close to the terminal methyl groups of DMPC, closer to the midplane of the membrane. Figure 2 illustrates such hypothetical membrane conformations and locations of **1**−**3**, respectively. Interestingly, since **3** does not exhibit significant cytotoxicity compared with **1** and **2**, from these observations the cytotoxicity profiles of the asimicin-type acetogenins would seem to be related to the membrane conformation of the acetogenins, i.e., the location of the lactone ring within the lipid bilayer may be important to elicit the protein interactions that maximize cytotoxicity. This is the first report of the elucidation of the conformation of Annonaceous acetogenins within membranes.

MATERIALS AND METHODS

Materials. All acetogenins tested, asimicin (**1**), parviflorin (**2**), longimicin B (**3**), and bullatacin (**4**) (Figure 1), were isolated and characterized in our laboratory as described elsewhere (*3*, *4*). Because the amount of **3** available was small, the DSC study on this compound was not carried out. Compound **4** is the 24-epimer of **1**, is relatively abundant, and thus was used for the measurement of the partition coefficient. Both perdeuterated (D-67: all deuterated except for the glycerol backbone) and nondeuterated DMPC were purchased from Avanti Polar Lipids and used as received. Manganese chloride ($MnCl_2$) was purchased from Aldrich. Deuterium oxide (D_2O), deuterated chloroform ($CDCl_3$), and tetramethylsilane (TMS) were purchased from Andover. Thin-layer chromatography (TLC) plates (K6F silica gel 60 Å) were purchased from Whatman.

Lipid Dispersions. DMPC films were dried on the surface of a round bottom flask from organic solvent solutions of the phospholipids by rotary evaporation at 45 °C for at least 24 h (*26*). The acetogenin was added to the organic solvent solutions with the phospholipids. MLVs for DSC studies were prepared by adding D_2O and vortexing at a lipid

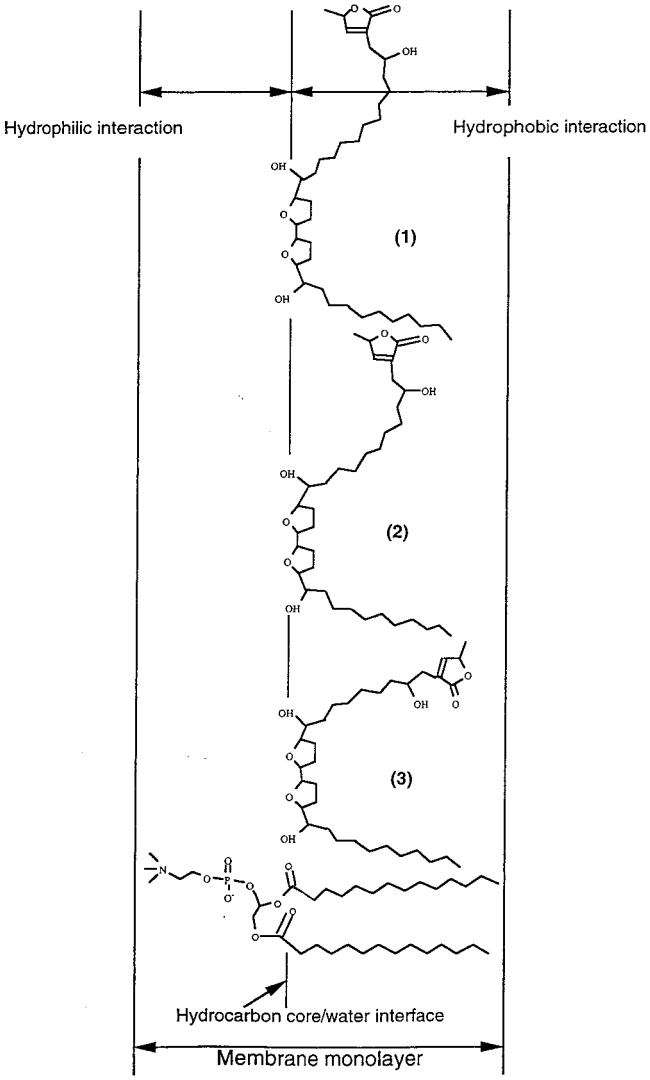

FIGURE 2: Hypothetical bulk conformations and locations of asimicin (**1**), parviflorin (**2**), and longimicin B (**3**) in the membrane.

concentration of ~100 mg/mL. SUVs for ^{1}H NMR studies were prepared by vortexing followed by probe sonication at a lipid concentration of ~5−15 mg/mL. The liposomes were left to stand at a temperature above the transition temperature (T_m) of the liposome samples for at least 2 h. They were then ultracentrifuged to sediment undesired lipid and MLVs and to remove particles of titanium released from the probe. TLC, using silica gel plates developed with chloroform/methanol/water (65:25:5), was used to evaluate lipid degradation; no degradation during sonication was found using 5% phosphomolybdic acid solution in 95% ethanol to visualize the phospholipids and acetogenins.

Samples with Mn^{2+} Preparation. To prepare the sample containing Mn^{2+}, 200 μL of the sonicated perdeuterated DMPC with an acetogenin dispersion was diluted with 150 μL of 90 mM NaCl solution containing 0.5 mM $MnCl_2$ (*27*). For the control sample, 200 μL of the sonicated perdeuterated DMPC with an acetogenin dispersion was diluted with 150 μL of 90 mM NaCl solution.

NMR Spectroscopy. The ^{1}H NMR spectra were recorded on a Varian VXR 500s spectrometer. Shigemi tubes were utilized to minimize the sample amount. The chemical shifts were measured relative to an internal terminal methyl peak of DMPC at 0.89 ppm. The sample temperature during all experiments was 40 °C, which is above the T_m of the liposome samples examined. For one-dimensional NOE experiments, a saturating field strength between 23 and 27 Hz was used.

For truncated NOE experiments, nondeuterated DMPC dispersions were used to observe intermolecular NOE (between DMPC and an acetogenin), and the concentration of the acetogenin was 20 mol % (*19*, *20*, *28*). Acquisitions of control spectra and spectra with individual saturated resonances were alternated. The recycle delay time was 3 s. The mixing times used were 0, 0.01, 0.02, 0.05, 0.07, 0.1, and 3 s. Finer increments were employed for shorter mixing times. Sixteen or 32 transients were acquired in each experiment. The growth curves of each peak with variable irradiation times were obtained and were described as the percentage of growth of NOEs, that is, $\eta(t)/\eta(3) \times 100$ (%), where $\eta(t)$ is the intensity of an NOE at a preirradiation time t, and $\eta(3)$ is its steady-state value (3-s irradiation). The initial buildup rates, i.e., the slopes of the curves at the initial stages, were calculated using least-squares regression methods.

For all other experiments, perdeuterated DMPC (D-67) dispersions were used. The concentration of the acetogenin was 10 mol % for difference NOE experiments, two-dimensional NOE spectroscopy (NOESY) experiments, and Mn^{2+} experiments. The mixing time (τ_m) was set at 100 ms in all difference NOE experiments. The spectral width of 4 kHz was used, and transmitter offset (TOF) was set at the HDO resonance. Decoupler offsets (DOF) were set on the peak of interest and at 2000 Hz as a control, which is out of the spectral window. Acquisitions of control spectra and spectra with individual saturated resonances were alternated. The recycle delay time was 3 s. Thirty-two transients were collected, and a 10-Hz exponential window function was used before Fourier transformation.

NOESY experiments were carried out in the phase-sensitive mode. The NOESY pulse sequence ($\Pi/2-t_1-\Pi/2-\tau_m-\Pi/2-t_2$) was used with a τ_m of 80 ms (*20*). The transmitter was set on the HDO resonance, and a 3-s presaturation was used to suppress the HDO resonance; 128 t_1 increments with 16 transients per increment were used. In t_2, 2K data points were acquired over a spectral width of 5 kHz with a 3-s recycle time. All spectra were processed on a SUN Sparc station. The data sets were multiplied by a Gaussian weighting function in both dimensions and zero-filled to 2K data points in the t_1 dimension before Fourier transformation.

Mn^{2+}-broadening experiments were carried out using a single 90° pulse and a 3-s repetition delay time (*27*, *29*). Solvent suppression was achieved by irradiation of the HDO resonance during the relaxation delay. The ^{1}H NMR spectra of sonicated dispersions were obtained from 32 or 64 transients, and a 10-Hz exponential window function was used before Fourier transformation.

Measurement of T_m. The T_ms of the dispersions of DMPC with asimicin (**1**)/parviflorin (**2**) were measured by DSC using MLVs on a Perkin-Elmer differential scanning calorimeter equipped with a thermal analysis data station. Four samples with different acetogenin concentrations (3, 5, 10, and 20 mol %) were tested for each compound. A heating scan rate of 10 °C/min was used.

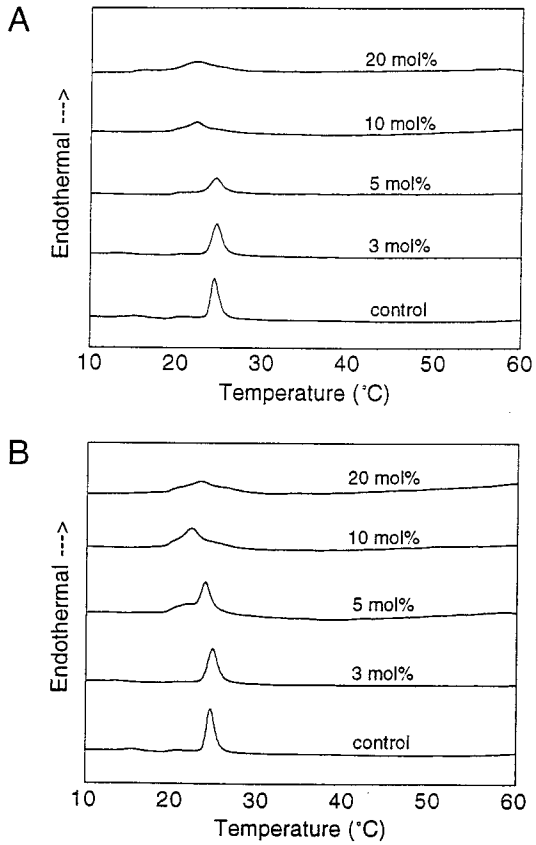

FIGURE 3: Thermograms of DMPC in the presence of different concentrations of acetogenins. A, DMPC with asimicin (**1**) dispersions; B, DMPC with parviflorin (**2**) dispersions.

Measurement of Partition Coefficients. Partition coefficients of bullatacin (**4**) employing octanol/water and octanol/water with Mn^{2+} were attempted using the shake flask method (*30*). Octanol was washed three times with equal volumes of water or Mn^{2+}-containing solution (0.25 mM $MnCl_2$ in water) prior to the experiments. Then 3 mL of octanol saturated with water was added to 3 mL of filtered water or a Mn^{2+}-containing solution with 5 mg of **4** in a centrifuge tube. Aliquots of the sample were carefully withdrawn from both phases and appropriately diluted for subsequent analysis by normal phase high-performance liquid chromatography (HPLC) using a silica gel column (DYNAMAX 60 Å R0008311C, Rainin) at 225 nm at ambient temperature. The aqueous phase was partitioned with dichloromethane (CH_2Cl_2), which is the solvent used for fractionation of acetogenins (*1*). All of **4** should partition into the CH_2Cl_2 phase. The mobile phase was methanol (9% v/v) and THF (1% v/v) in hexane. The presence of bullatacin in aliquots was also checked using a Beckman DU-600 spectrophotometer.

RESULTS

DSC Studies. DSC has been used to measure the strength of drug−phospholipid interactions (*31*). Parts A and B of Figure 3 represent the endotherms of DMPC in the presence of **1** and **2**, respectively. Both **1** and **2** exhibit similar profiles in their DMPC thermograms. As the concentrations of these acetogenins increase, the T_m peak becomes broader, and the T_m maximum is shifted slightly to lower temperature. The calorimetric enthalpy is relatively constant. Drugs with such an interaction profile are thought to be partially buried in the hydrocarbon core of the bilayer, and they interact mainly with the glycerol backbone and the head group of phosphatidylcholine (*25*).

Table 1: Calculated Distances between Two Chemical Groups Based on Truncated NOE Results Using Equation 3[a]

compound	irradiated chemical group	chemical groups <3.6 Å	chemical groups ≤3.6 Å
asimicin (**1**)	*e*	*d*, III	*c*, *g*, *h*, *i*, I
	i	*g*, *h*	*a*, *c*, *d*, *e*, I, III
	d	*c*, *e*, *g*, I, III	*a*, *h*, *i*
	a	*c*, *d*, *e*, *g*, I, III	*h*, *i*
parviflorin (**2**)	*e*	*c*, *d*, *g*, I, III	*a*, *h*, *i*
	i	*g*, *h*	*a*, *c*, *d*, *e*, I, III
	d	*c*, *e*, *g*, III	*a*, *h*, *i*, I
	a	*c*, *e*, III	*d*, *g*, *h*, *i*, I
longimicin B (**3**)	*e*	*c*, *d*, I, III	*a*, *g*, *h*, *i*
	i	*g*, *h*	*a*, *c*, *d*, *e*, I, III
	d	*c*, *e*, III	*a*, *g*, *h*, *i*, I
	a	*c*, *d*, I, III	*e*, *g*, *h*, *i*

[a] The reference distance used for distance calculations was the distance between *a* and *c* of DMPC. The chemical group assignments are shown in Table S 2.

In ^{1}H NMR spectra, all three asimicin-type acetogenins (**1**−**3**) tested in this study showed the same chemical shift pattern as shown in Table 1 (*32*). The only structural differences among these compounds are the length of the alkyl chain between the lactone ring and the THF rings, which are 15, 13, and 11 carbons, respectively for **1**−**3**, as shown in Figure 1. The total carbon chain lengths and molecular weights of **2** and **3** are the same (32 carbons), but the THF ring locations are shifted. Compounds **1** and **3** have the same alkyl chain length between the THF rings and the terminal methyl groups, but the alkyl chain between the lactone ring and the THF rings of **3** is four carbons shorter than that of **1**. Acetogenin **2** has an alkyl chain that is two carbons shorter between the lactone ring and the THF rings than it is in **1**. ^{1}H NMR of these compounds shows minor differences in the integrations for the peaks of the alkyl methylene protons, but these are sometimes difficult to estimate. Thus, the structure determinations of these compounds were accomplished using mass spectrometry (*4*). ^{1}H NMR assignments of the acetogenins in DMPC dispersions were made by comparing ^{1}H spectra of acetogenins in $CDCl_3$, dispersions of DMPC with acetogenin, and dispersions of DMPC without acetogenin. Besides the comparisons between the ^{1}H spectra, the chemical shifts of the acetogenins were confirmed by ^{1}H two-dimensional NMR experiments. The chemical shift assignments for DMPC and the acetogenins observed in DMPC dispersions are shown in Table S 2 (Supporting Information). All chemical shifts in dispersions are referenced to the internal terminal methyl peak (*i*) of DMPC at 0.89 ppm. The chemical group assignments of DMPC and the acetogenins are shown in Figure 1.

Five ^{1}H NMR peaks due to the acetogenins were identifiable in the DMPC dispersion system. Spectra in undeuterated (**A**) and perdeuterated (**B**) DMPC are shown in Figure 4. The peak intensities of the acetogenins in a nondeuterated DMPC system are relatively low compared with those of DMPC because the concentration of acetogenins was 5 times lower than that of DMPC. However, in the perdeuterated DMPC, the peak intensities of acetogenins are comparable

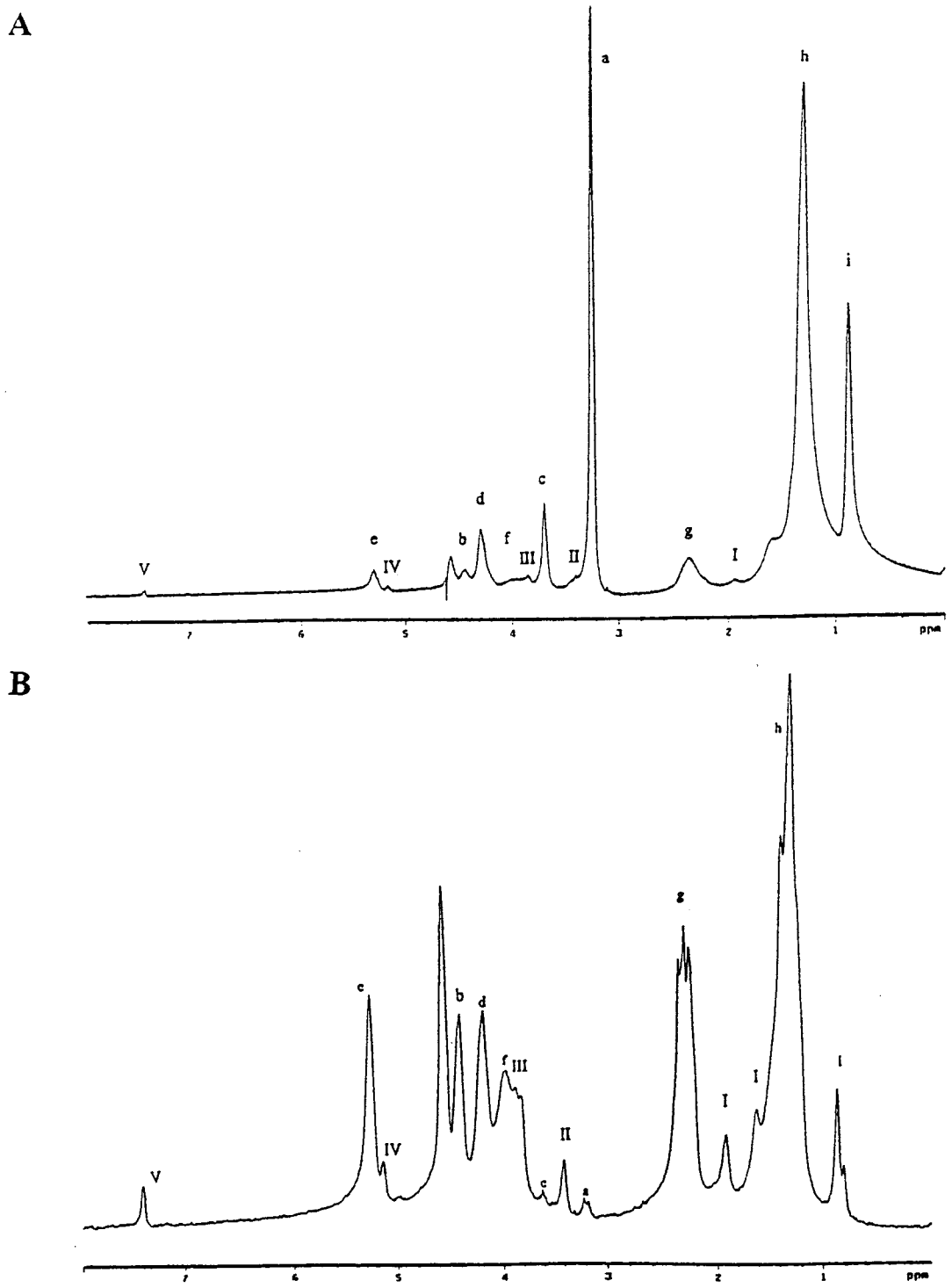

FIGURE 4: ^{1}H NMR spectra of **A**, DMPC with asimicin dispersions; **B**, perdeuterated lipid D-67 with asimicin dispersions. The peak assignments are listed in Table S 2.

to the residual bilayer peaks. The concentration of acetogenins was 10 times lower than that of perdeuterated DMPC. The splittings resolved in the DMPC peaks seen in part **B** of Figure 4 were caused by chemical shift differences between residual protons. The same splittings were observed in control dispersions of D-67 alone. The acetogenin peak at 1.95 ppm (also at 1.60 ppm observed in D-67 dispersions) in lipid dispersions was designated as peak I. Similarly, the peak at 3.41 ppm was designated as peak II; the peak at 3.86 ppm, as peak III; the peak at 5.17 ppm, as peak IV; and the peak at 7.43 ppm, as peak V. As shown in Figure 4, significant line broadening was observed in the ^{1}H NMR spectra of the DMPC dispersions. The sonicated vesicles tumble slowly, dipolar coupling is not fully averaged, and line broadening is the consequence. Also, the *J* couplings observed in ^{1}H NMR spectra of acetogenins in $CDCl_3$ solution could not be resolved in a spectrum of dispersions of DMPC with acetogenin.

Attempts to measure the partition coefficient of bullatacin (**4**) using octanol/water and octanol/aqueous Mn^{2+} solution failed because none of the acetogenin was detected in the aqueous layers using HPLC (detection limit $\sim 10^{-9}$ M). The

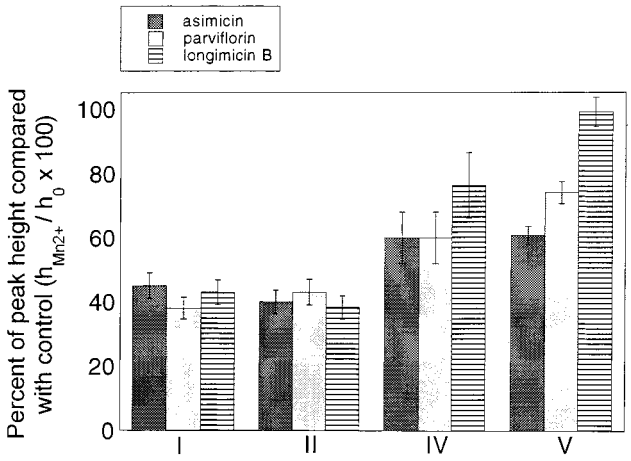

FIGURE 5: Percents of peak heights [$h_{(Mn^{2+})}/h_0 \times 100$) of asimicin (**1**), parviflorin (**2**), and longimicin B (**3**) compared with heights in the absence of the Mn^{2+} ions (h_0) in the dispersions. The peak assignments are listed in Table S 2.

presence of **4** in aliquots was also examined using a spectrophotometer. Bullatacin (**4**) (λ_{max} = 228 nm) was detected only in octanol fractions giving a partition function $>10^9$. No ^{1}H NMR signals were observed when acetogenin alone was dispersed in D_2O. Thus, only membrane-accessed acetogenins can be observed in ^{1}H NMR spectra.

^{1}H NMR spectra of acetogenin (20 mol %) dispersion in DMPC solution were integrated and showed a 5:1 ratio between well-isolated DMPC peaks and acetogenin peaks. The acetogenin ^{1}H peaks at high field (~0.9−1.8 ppm) heavily overlapped peaks of the DMPC acyl chains (*h* and *i*). Thus, no peak assignments were made for the acyl chain regions of the acetogenins. Nevertheless, five peaks of the acetogenins were clearly assigned, two peaks from the lactone region and three peaks from the THF ring region. These observations were fortunate because the locations of the THF rings and the lactone ring were key pieces of information needed to solve the location and the conformation of these acetogenins in the bilayer membranes.

Mn^{2+} Broadening. For chemical groups that are close to Mn^{2+} (the electron−nuclear dipole interaction is effective at about 5−10 Å), the ^{1}H NMR spectral peaks are significantly broadened or eliminated. The width of the bilayer membrane is roughly 40 Å. Thus, for a chemical group close to the interface, the spectral peaks will be broadened; for a chemical group close to the midplane, the spectral peaks will remain the same. We chose the peak height of *i* (terminal methyl group of DMPC) for reference as it was assumed it would not change on addition of Mn^{2+}. The peak height ratios of **1**−**3** with and without Mn^{2+} are compared in Figure 5. The peak height ratios were in the order V > IV > I ≥ II. Peak V decreased in spectral peak height by 40%; peak I, by 55%; peak IV, by 40%; and peak II, by 60% in dispersions of compound **1** in D-67. Peaks of both the lactone ring and the THF rings of **1** broadened; however, the peaks of the THF rings broadened more than those of the lactone ring. The same trend is true in dispersions of **2** in deuterated bilayers. Peak I decreased in spectral intensity by 60%; peak II, by 60%; peak IV, by 40%; and peak V, by 25%. Peak I decreased in spectral peak height by 60%; peak II, by 60%; peak IV, by 25%. Peak V was virtually the same peak height as the control in D-67 with **3** dispersions. The peaks of *a* and *e* of DMPC were broadened by 80% and 65%, respectively, after the addition of Mn^{2+}.

Difference NOE. Difference ^{1}H NMR NOE experiments were carried out with dispersions of acetogenin in deuterated DMPC (D-67). All NOEs shown were negative as the dispersions were in the slow tumbling regime. Figures 6−8 show NOE difference spectra for irradiations of the lactone proton peak V and the carbinol proton peak II of acetogenins. Spectrum B in Figure 6 shows the NOE difference spectrum of dispersions of **1** in D-67 when the THF protons II were irradiated. It clearly shows that there are NOE correlations between II and the head group of DMPC (*d*, *e*, *f*, and *g*) as well as NOE correlations between II and the other peaks of the THF rings (I and III). Spectrum A in Figure 6 shows the NOE spectrum of the same dispersions when the lactone proton V was irradiated. In the spectrum of dispersions of compound **1** in D-67, peak V did not have any correlation with peaks of the head group of DMPC but only with the acyl chain region of DMPC (*h* and *g*). As shown in Figure 7, the results of dispersions of compound **2** in D-67 showed a pattern similar to that of dispersions of compound **1** when II was irradiated; correlations were apparent with the head group of DMPC and the other THF ring peaks. The irradiation of V caused a correlation with the acyl chain of DMPC (*h*) and none with the α methylene groups (*g*). Spectra A and B in Figure 8 show the difference NOE spectra of dispersions of compound **3** in D-67 in which V and II were irradiated, respectively. Irradiation of II caused NOE buildups of the peaks of the head groups of DMPC and the other peaks of the THF rings. In contrast with the results of dispersions of compounds **1** and **2**, an irradiation of V in dispersions of compound **3** caused NOE correlations between V and the terminal methyl groups (*i*) and the acyl methylene groups of DMPC (*h*).

NOESY. The NOESY spectrum of dispersions of compound **1** in D-67 is shown in Figure 9. Since the intermolecular cross-peaks observed were of the THF rings but not of the lactone ring of acetogenins, all compounds studied showed the same results, i.e., the THF ring peaks of all compounds studied had cross-peaks with the glycerol backbone of DMPC. The cross-peaks between peak II and the peaks of the glycerol backbone are clearly seen. The cross-peaks between peak III and the peaks of the glycerol backbone are difficult to distinguish from those between *f* and the other glycerol backbone peaks. However, it is clearly seen that III has a strong correlation with *g* of DMPC. The peaks of the THF ring regions have strong intramolecular correlations and intermolecular correlations with the head group of DMPC. No clear cross-peaks were observed in the NOESY spectra between the lactone ring peaks (IV and V) and the DMPC peaks in this experiment.

Truncated NOE. The time dependence of several NOEs were examined. The growth of NOEs for **1**−**3**, when four different peaks of DMPC (peaks *e*, *i*, *d*, and *a*) were saturated, are shown in parts a−d, respectively, of Figures 10−12. Even though the five peaks of the acetogenins (peaks I−V) were assignable in the ^{1}H NMR spectra of dispersions of DMPC with acetogenin, the peak intensities of the protons at the lactone ring (IV and V) and the protons at the carbons next to the THF rings (II) of the acetogenins were too low for accurate mesurement. Thus, only two peaks from the THF ring region (I and III) were examined in truncated NOE

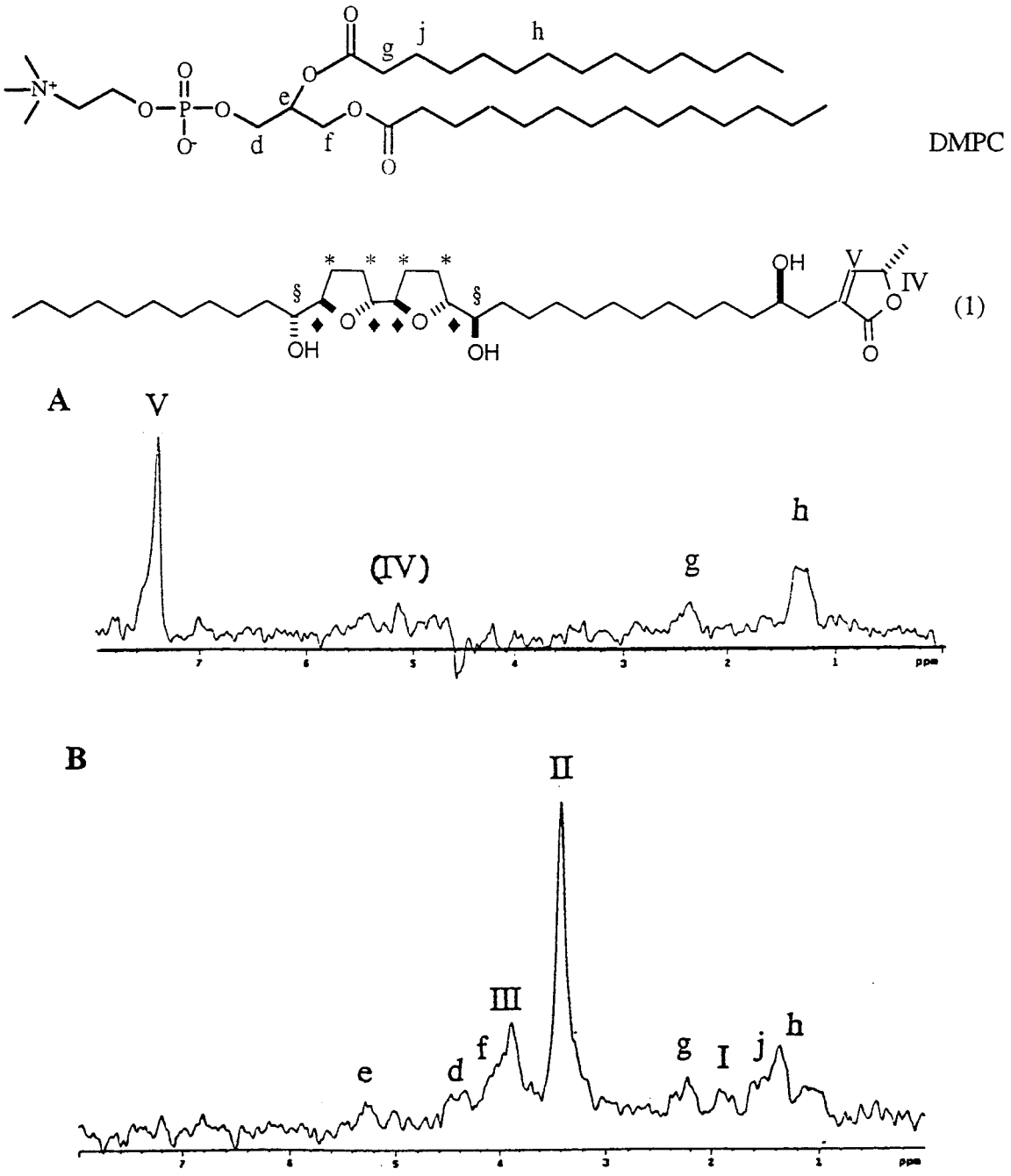

FIGURE 6: 1H NMR difference NOE spectrum of perdeuterated lipid D-67 with asimicin (**1**) dispersions. The peak assignments are listed in Table S 2. **A**, irradiation of V; **B**, irradiation of II. The control spectrum (DOF = 2000 Hz) was subtracted from the spectrum with an irradiation of V/II. I: *, II: §, III: ◆.

experiments, and changes in the NOE at resonances of these peaks were monitored. Negative NOEs were observed due to the long correlation times arising from slow tumbling of the DMPC vesicles. In part a of Figure 10, the overall ordering was III > *d* > *g* > I > *a* > *h* > *i* from highest to lowest buildup rates when the proton of the methine groups in the glycerol backbone (*e*) was saturated. This shows that both proton peaks I and III of the THF rings of **1** have higher buildup rates than the acyl chains (*h*) and the terminal methyl groups (*i*) of DMPC when the proton of the glycerol backbone of DMPC is saturated. This observation agrees with the data shown in parts B−D of Figure 11. In part B of Figure 10, the overall ordering was *h* >> *g* > *e* > *d* ≈ *a* > *c* > III ≈ I, which clearly shows that both peaks I and III of **1** have very low buildup rates compared with that of the acyl chains of DMPC (*h*). In parts c and d of Figure 10, the percentages of growth of NOEs during saturations of *d* and *a* , respectively, show similar trends as in part a, i.e., both peaks I and III of **1** have higher buildup rates than the acyl chains and the terminal methyl groups of DMPC (*h* and *i)* when a peak of the head groups of DMPC is saturated. These observations support the conclusion that the differences in buildup rates are not the results of spin diffusion effects but rather the results of larger dipole couplings and shorter interproton distances. Similar to Figure 10 for compound **1**, Figures 11 and 12 show the percentages of growth of NOEs with **2** and **3**, respectively. Both **2** and **3** showed virtually the same results as **1**, i.e., peaks I and III

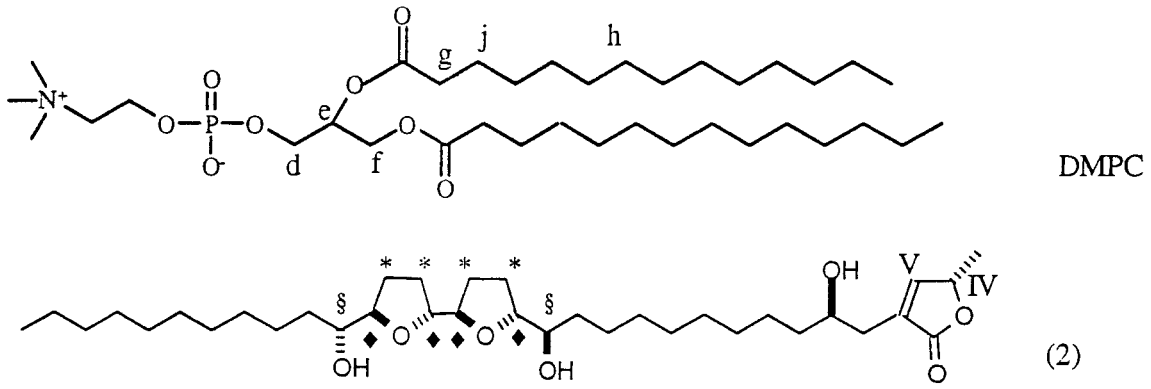

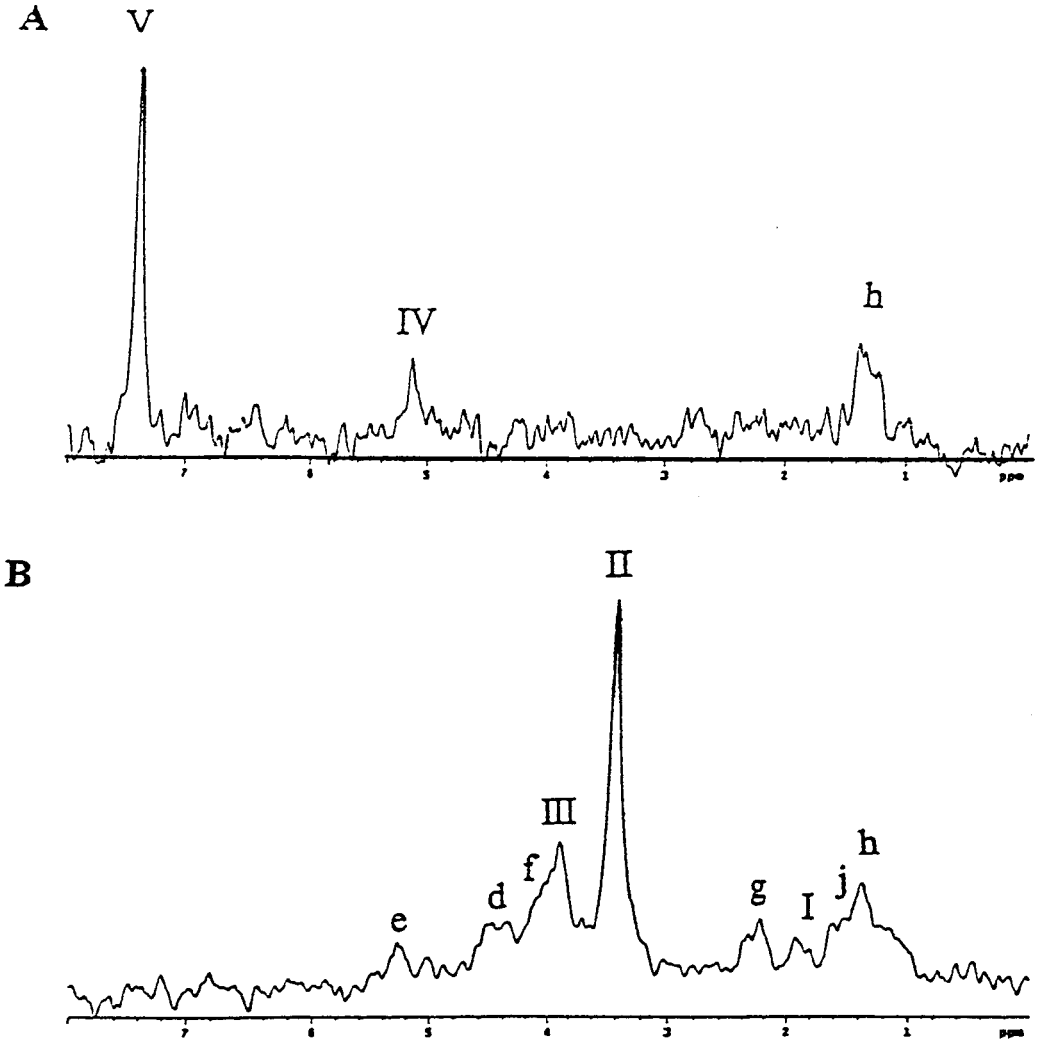

FIGURE 7: 1H NMR difference NOE spectrum of perdeuterated lipid D-67 with parviflorin (**2**) dispersions. The peak assignments are listed in Table S 2. **A**, irradiation of V; **B**, irradiation of II. The control spectrum (DOF = 2000 Hz) was subtracted from the spectrum with an irradiation of V/II. I: *, II: §, III: ◆.

of the THF rings of **2** and **3** had higher NOE buildup rates than did those of the acyl chains and the terminal methyl groups of DMPC (*h* and *i*) when a peak of the head groups of DMPC (*e*, *d*, or *a*) was saturated but lower buildup rates when the terminal methyl peak of DMPC (*i*) was saturated.

DISCUSSION

Throughout this study, significant line broadening was observed in ^{1}H spectra of DMPC dispersions due to the size of the sonicated vesicles. As the radius of spherical vesicles increases, the lateral diffusion of individual phospholipid molecules in the bilayer becomes the relevant correlation time rather than the random reorientation of the vesicle as a whole. This limitation is the main reason why micelles with a radius of ~20−25 Å, have been more popular for NMR studies of this kind than liposomes whose minimum radius is about 120 Å. However, the packing of micelles is very different from that of bilayer vesicles. For the lipid

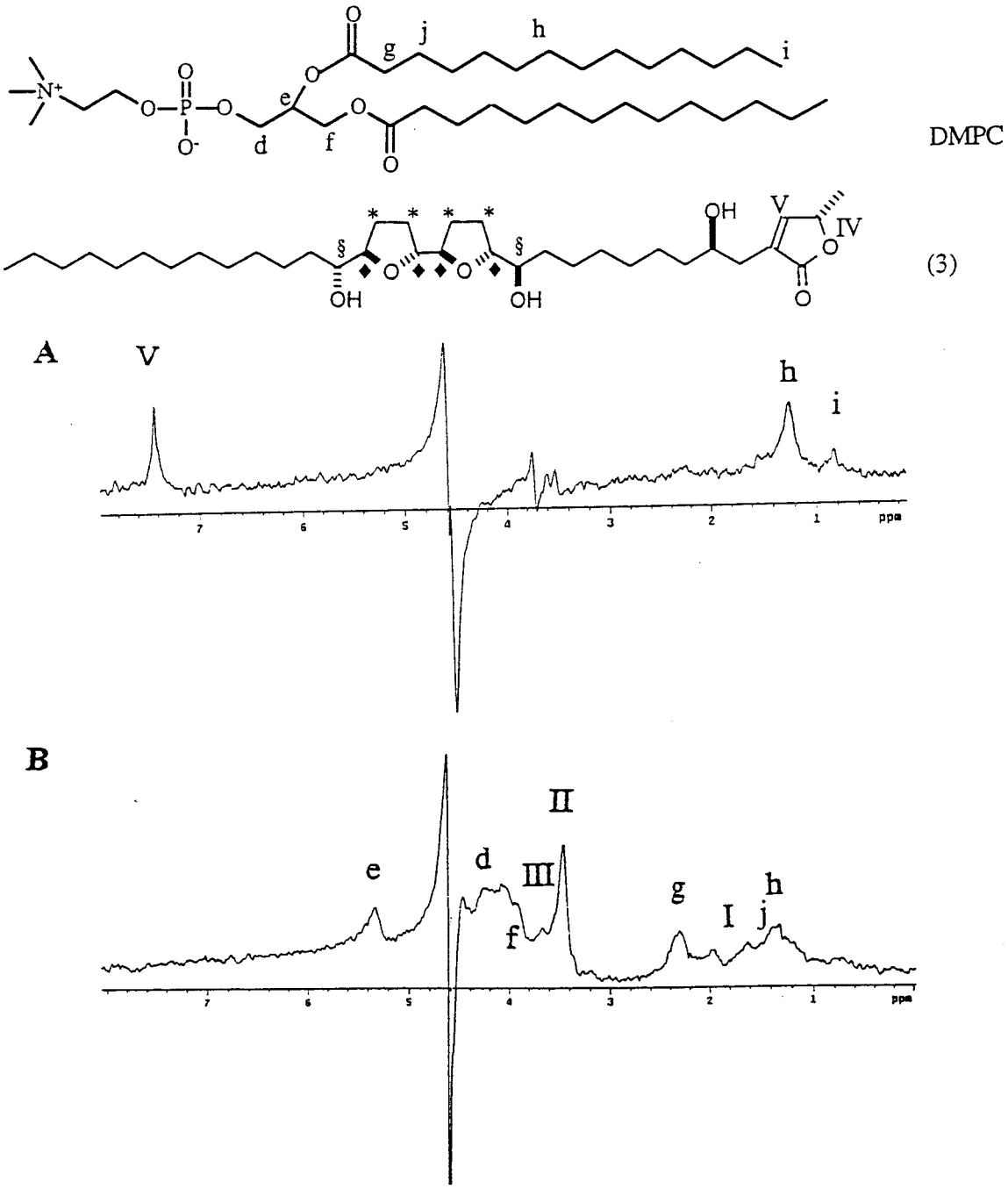

FIGURE 8: 1H NMR difference NOE spectrum of perdeuterated lipid D-67 with longimicin B (**3**) dispersions. The peak assignments are listed in Table S 2. **A**, irradiation of V; **B**, irradiation of II. The control spectrum (DOF = 2000 Hz) was subtracted from the spectrum with an irradiation of V/II. I: *, II: §, III: ◆.

dispersion systems studied here, NOE buildup curves are a powerful technique as they depend on the cross-relaxation rate rather than spin diffusion (*33*, *34*).

Ideally, only cross-relaxation determines the initial buildup rates (*33*). The rate of change of the *z* component of spin *I* (I_z) with time (t) on the saturation of spin *S* in a multispin system is given by

$$dI_z/dt = -R_I(I_z - I^0{}_z) - \sigma_{IS}(S_z - S^0{}_z) - \sum_X \sigma_{IX}(X_z - X^0{}_z) \quad (1)$$

where R_I is the spin relaxation rate of spin *I* due to other spins, σ_{IS} is the cross-relaxation rate between spins *I* and *S*, and σ_{IX} is the cross-relaxation rate between spins *I* and *X*. At $t = 0$, $X_z = X^0{}_z$, $I_z = I^0{}_z$, and $S_z = 0$, so that, from eq 1, the initial rate is

$$dI_z/dt|_{t=0} = \sigma_{IS} S^0{}_z \quad (2)$$

Right after *S* is saturated, cross-relaxation at a rate σ_{IS} starts, but the relaxation of *I* at a rate R_I begins significantly only at later times. The cross-relaxation rate in the homonuclear case can be estimated as

$$\sigma_{IS} = \left(\frac{\mu_0}{4\pi}\right)^2 \frac{\hbar^2\gamma^4}{10}\left(\frac{6\pi}{1+4\omega^2\tau_0{}^2} - \tau_0\right) r_{IS}{}^{-6} \quad (3)$$

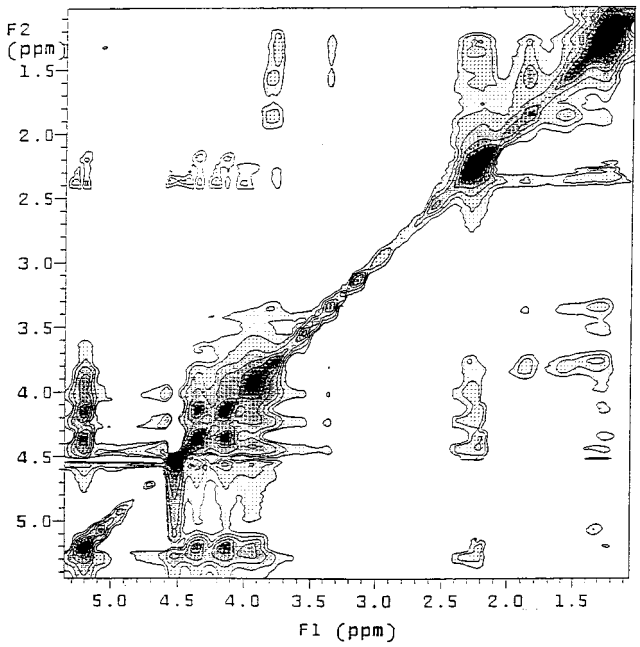

FIGURE 9: ^{1}H NOESY spectrum of perdeuterated lipid D-67 with asimicin (**1**) dispersions.

where μ_0 = permeability constant, $\hbar$ = Plank's constant, γ = magnetogyric ratio of proton, ω = Larmor frequency, r_{IS} = distance between spin I and S, τ_0 = correlation time for the coupled dipoles. There are two variables, r_{IS} and τ_0, in eq 3. Motions in the liposome system are divided into three classes: random reorientation of the vesicle as a whole ($\sim 10^{-3}$ s), lateral diffusion of the individual molecules ($\sim 10^{-8}$ s), and the phospholipid's torsional motion (10^{-3}–10^{-9}) (*35*, *36*). In the NMR time scale, the phospholipid's torsional motion is for proton dipolar interactions in typical phospholipids, i.e., the correlation time and τ_0 can be assumed to be constant (*20*, *37*, *38*). Thus, σ_{IS} is proportional to r_{IS}^{-6}, i.e., the initial buildup rate of the NOE enhancement is proportional to r_{IS}^{-6}. The rate at which the slope of the NOE buildup curve falls away from linearity depends on spin diffusion and the spin−lattice relaxation rate of I. For liposome systems, which have very short relaxation times, the linearity of the NOE buildup curve is limited to short mixing times (*19*, *20*, *28*, *31*). Spin diffusion effects are inevitable in these lipid dispersions. Therefore, the comparison of buildup rates for estimation of contact points is valid only during a period that is short enough relative to the rate of spin diffusion in liposome systems.

The distances between two chemical groups from the NOE buildup results were calculated using eq 3. The distance between the chemical groups *a* and *c* of DMPC was estimated as 3.4 Å. Then this was used as a reference distance to determine other distances by comparing the slopes of the buildup curves based on eq 3. It was revealed that all distances calculated were in the range of 3−6 Å, around 5 Å is the maximum detectable lipid distances due to spin diffusion effects. Nonetheless, the calculated distances could be divided into two groups: less than 3.6 Å, and more than 3.6 Å, as summarized in Table 1. Although I must have a buildup rate similar to that of III (both I and III are from the THF ring region), I tended to show a buildup curve rate between III and *h* because I includes contributions from *h* due to partial peak overlap. It was clearly shown that, even though lipid dispersion systems suffer from spin diffusion,

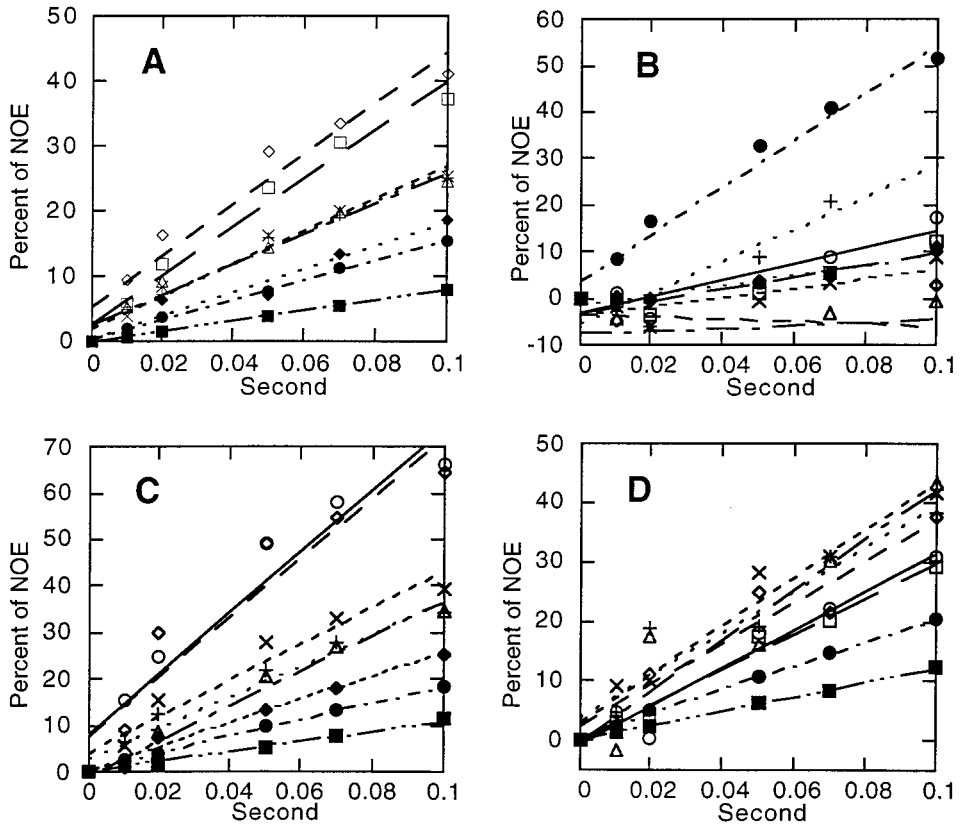

FIGURE 10: Percentage of growth of ^{1}H NOEs for DMPC with asimicin (**1**) dispersions during **A**, irradiation of *e*; **B**, irradiation of *i*; **C**, irradiation of *d*; **D**, irradiation of *a*. *e* (○); *d* (□); III (◇); *c* (X); *a* (◆); *g* (+); I (△); *h* (●); *i* (■). The peak assignments are listed in Table S 2.

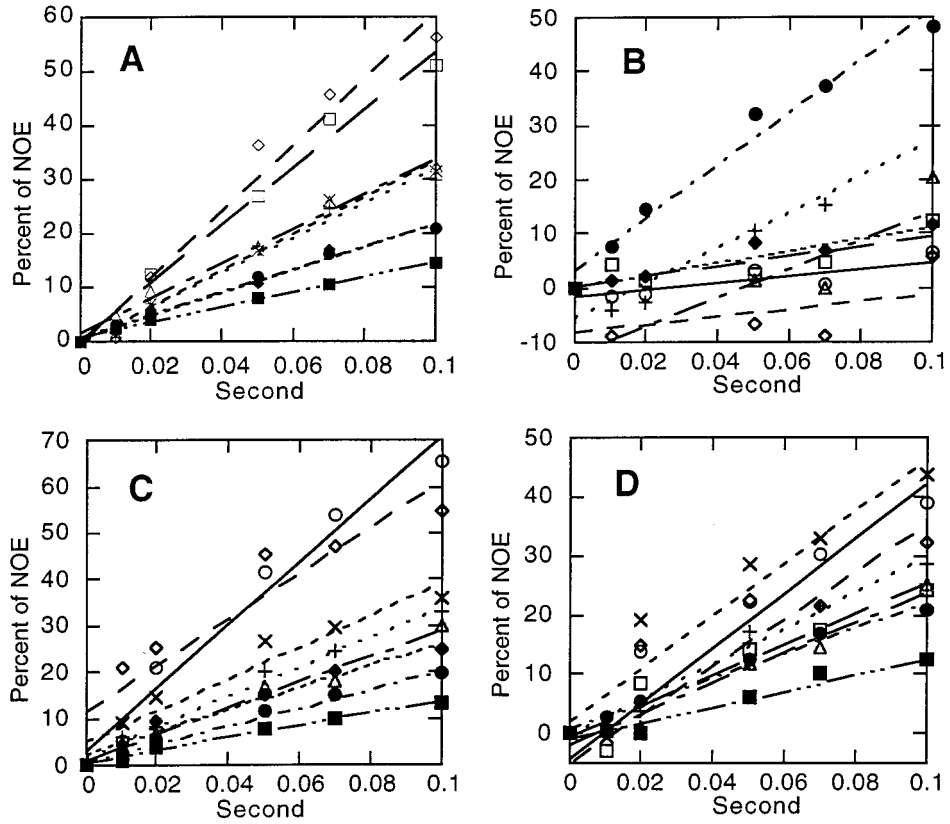

FIGURE 11: Percentage of growth of 1H NOEs for DMPC with parviflorin (**2**) dispersions during **A**, irradiation of *e*; **B**, irradiation of *i*; **C**, irradiation of *d*; **D**, irradiation of *a*. *e* (○); *d* (□); III (◇); *c* (X); *a* (◆); *g* (+); I (△); *h* (●); *i* (■). The peak assignments are listed in Table S 2.

measurements of the initial rates of NOE buildup curves match the known interproton distances.

From the truncated NOE experiments, the THF rings of each acetogenin reside near the polar interfacial head group region of the DMPC membranes. This conclusion was also supported by the NOESY experiments in which the THF rings gave strong correlations with the glycerol backbone region of DMPC. The DSC studies indicated that **1** and **2** exhibit a characteristic transition profile for amphiphilic compounds, which strongly interact with the glycerol backbone and the polar head group of the phospholipids (*25*).

In the NOESY experiments, there was no strong cross-peak between the lactone peaks (V and IV) and DMPC. This suggested that the lactone rings might not have as well-defined a location in the membrane as the THF rings or that the cross-peak intensities were not high enough to be seen in a two-dimensional spectrum. To investigate the lactone ring peaks specifically, difference NOE experiments were conducted, and **1**−**3** exhibited different NOE buildup profiles. For compound 1, which has the longest alkyl chain length between the THF rings and the lactone ring of the three compounds tested, the NOE buildup data indicate that the lactone ring showed the NOE buildup with α-methylene groups (*g*) just below the interfacial region of DMPC. Acetogenin **2**, which has a two-carbon shorter alkyl chain length between the two ring systems, showed an NOE buildup with the lower acyl chain region rather than the α-methylene groups (*h*); this indicates that the lactone ring of **2** is located between the interfacial region and the midplane of the membrane. Compound **3**, which has a four-carbon shorter alkyl chain, showed NOE buildups with the terminal methyl groups of DMPC (*i*) and the methylene alkyl chain region of DMPC (*h*). These results suggest that the locations of the lactone rings of these asimicin-type acetogenins depend on the length of the alkyl chain between the THF rings and the lactone rings.

These observations are also mutually supported by the Mn^{2+}-broadening experiments; the proton signals for the THF rings of all acetogenins tested were broadened by addition of Mn^{2+}. This indicates that the THF rings are in the range of 10 Å from Mn^{2+}, i.e., closer to the polar head groups than to the midplane of the DMPC bilayer membranes. The lactone rings of **1** and **2** experienced less peak broadening than the THF rings of these compounds. This again suggests that the lactone rings of **1** and **2** are located closer to the interface than to the midplane of the membrane, but are below the THF rings. The lactone ring of **3** showed little effect in the presence of Mn^{2+}, which indicates that the lactone ring of **3** resides closer to the midplane of the membrane.

A number of compounds containing lactone rings have been reported to be cytotoxic (*39*−*41*). The reduction of the double bond in the lactone ring of bullatacin (**4**) (the C-24 epimer of **1**) caused a 10^7 reduction in cytotoxicity (*1*). Such results imply that the unsaturated γ-lactone subunit is crucial for the potent cytotoxicity of acetogenins. The current study indicates that the location of the lactone ring moiety of the asimicin-type acetogenins in the membrane is determined by the length of the alkyl chain between the THF rings and the lactone ring. Compound **3** exhibits at least 10^2 less cytotoxicity against multidrug-resistant cells (MCF-7/Adr) (*17*) and 10^9 less cytotoxicity against human colon

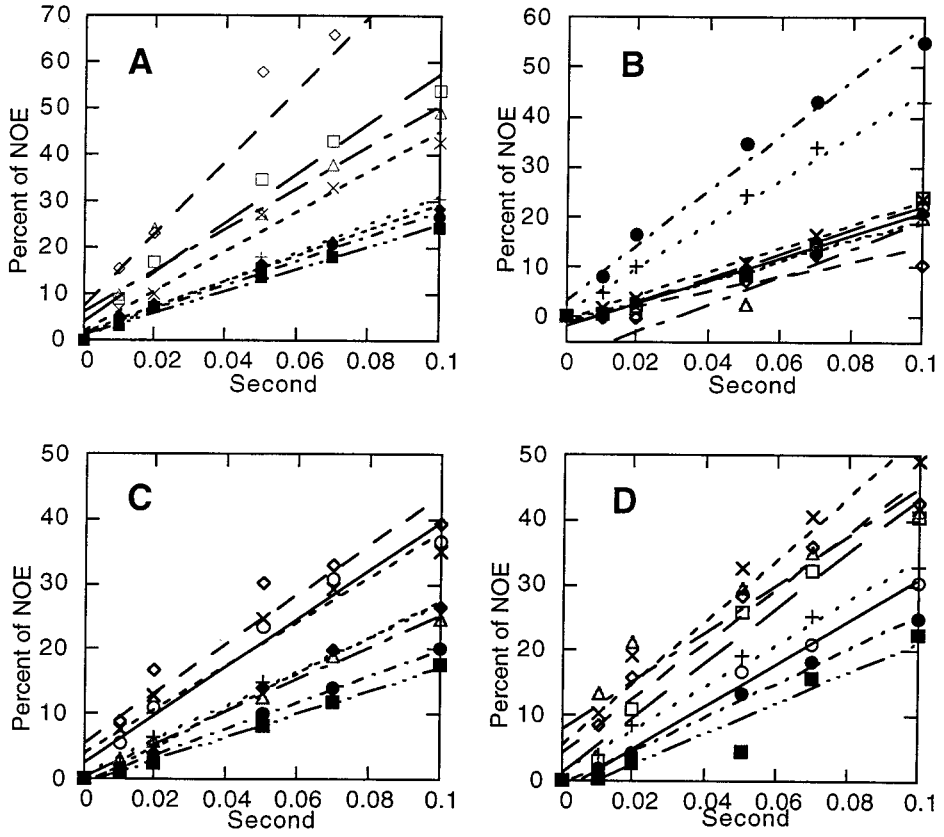

FIGURE 12: Percentage of growth of 1H NOEs for DMPC with longimicin B (**3**) dispersions during **A**, irradiation of *e*; **B**, irradiation of *i*; **C**, irradiation of *d*; **D**, irradiation of *a*. *e* (○); *d* (□); III (◇); *c* (X); *a* (◆); *g* (+); I (△); *h* (●); *i* (■). The peak assignments are listed in Table S 2.

adenocarcinoma cells (HT-29) (*42*) compared with **1**. Thus, the location of the lactone ring moiety in the lipid bilayer correlates well with the level of cytotoxicity. Although some acetogenins lacking THF rings are known to be cytotoxic, they are relatively much less potent, and the presence of the THF rings in the acetogenins certainly enhances their unique cytotoxic potency (*43*, *44*).

Considering the above data, we propose that the THF rings, with their flanking hydroxyl groups, act as a hydrophilic anchor in the lipid membrane. The position of the THF ring-anchor along the acetogenin chain determines the depth of the lactone functional group, which then directly acts with the protein receptor site(s), perhaps, mimicking the quinone ring of ubiquinone (*29*, *45*). The functional lactone group reaches the receptor site(s) by lateral diffusion in the membrane. The THF rings, acting as an anchor in the lipid bilayer, may thus enhance the bioactivity by restricting the location, conformation, and orientation of the functional lactone moiety by interacting with the head group of the phospholipid. Figure 2 illustrates such hypothetical conformations and membrane locations of **1**, **2**, and **3**, respectively.

One of the questions remaining to be answered is whether the hydrophilic interaction is intermolecular (i.e., between the glycerol backbone of DMPC and the THF oxygen/flanking hydroxyls of an acetogenin) or intramolecular (i.e., between the THF oxygen and the flanking hydroxyl groups within an acetogenin molecule). Most Annonaceous acetogenins with THF rings possess two flanking hydroxyl groups, and those that possess only one are usually less potent (*3*). These hydroxyl groups could create intramolecular hydrogen bonds with the oxygen in the adjacent THF ring and/or the other hydroxyl, and they could also experience interactions with the oxygens in the backbone of the phospholipid. A better understanding of the mode of action and the molecular geometry of the acetogenins within the lipid membranes of various cell types may help to establish useful therapeutic selectivities of this type of compounds.

ACKNOWLEDGMENT

The useful discussions with Dr. C. Pidgeon and help from the research group of Dr. S. Nail for the DSC studies are appreciated.

SUPPORTING INFORMATION AVAILABLE

Table S 1, ^{1}H NMR chemical shift assignments for asimicin-type compounds in $CDCl_3$; Table S 2, ^{1}H NMR chemical shift assignments for compounds **1**−**3** in $CDCl_3$ and sonicated DMPC dispersions with and without acetogenin (20 mol %); and chemical group assignments of DMPC and asimicin-type acetogenins in Figure 1 (2 pages). Ordering information is given on any current masthead page.

REFERENCES

1. Rupprecht, J. K., Hui, Y.-H., and McLaughlin, J. L. (1990) *J. Nat. Prod. 53*, 237−278.
2. Fang, X.-P., Rieser, M. J., Gu, Z.-M., Zhao, G.-X, and McLaughlin, J. L. (1993) *Phytochem. Anal. 4*, 27−67.
3. Gu, Z.-M., Zhao, G.-X., Oberlies, N. H., Zeng, L., and McLaughlin, J. L. (1995) in *Recent Advances in Phytochemistry* (Arnason, J. T., Mata, R., and Romeo, J. T., Eds.) Vol. 29, pp 249−310, Plenum Press, New York.

4. Zeng, L., Ye, Q., Oberlies, N. H., Shi, G., Gu, Z.-M., He, K., and McLaughlin, J. L. (1996) *Nat. Prod. Rep. 13*, 275−306.
5. Cavé, A., Figadère, B., Laurens, A., and Cortes, D. (1997) *Prog. Chem. Org. Nat. Prod. 70*, 81−273.
6. Ahammadsahib, K. I., Hollingworth, R. M., McGovren, J. P., Hui, Y.-H., and McLaughlin, J. L. (1993) *Life Sci. 53*, 1113−1120.
7. Friedrich, T., Van Heek, P., Ohnishi, T., Forche, E., Kunze, B., Jansen, R., Trowitzench-Kienast, W., Hofle, G., Reichenbach, H., and Weiss, H. (1994) *Eur. J. Biochem. 219*, 691−698.
8. Morré, J. D., DeCabo, R., Farley, C., Oberlies, N. H., and McLaughlin, J. L. (1995) *Life Sci. 56*, 343−348.
9. Anderson, J. E., Goetz, C. M., and McLaughlin, J. L. (1991) *Phytochem. Anal. 2*, 107−111.
10. Yu, J.-G., Hu, X. E., Ho, D. K., Bean, M. F., Stephens, R. E., and Cassady, J. M. (1994) *J. Org. Chem. 59*, 1598−1599.
11. Trunbore, M., Chester, D. W., Moring, J., and Rhodes, D. (1988) *Biophys. J. 54*, 535−543.
12. Mason, R. P., Rhodes, D. G., and Herbette, L. G. (1991) *J. Med. Chem. 34*, 869−877.
13. Mason, P. R., Campbell, S. F., Wang, S.-D. , and Herbette, L. G. (1989) *J. Mol. Pharmacol. 36*, 634−640.
14. Landolt, J. L., Ahammadsahib, K. I., Hollingworth, R. M., Barr, R., Crane, F. L., Buerck, N. L., McCabe, G. P., and McLaughlin, J. L. (1995) *Chem.-Biol. Interact. 98*, 1−13.
15. Alfonso, D. A., Johnson, H. A., Colman-Saizarbitoria, T., Presley, P. P., McCabe, G. P., and McLaughlin, J. L. (1996) *Nat. Toxins 4*, 181−188.
16. He, K., Zeng, L., Ye, Q., Shi, G., Oberlies, N. H., Zhao, G.-X., Njoku, C. J., and McLaughlin, J. L. (1997) *Pestic. Sci. 49*, 372−378.
17. Oberlies, N. H., Croy, V. L., Harrison, M. L., and McLauglin, J. L. (1997) *Cancer Lett. 115*, 73−79.
18. Oberlies, N. H., Chang, C. -J., and McLaughlin, J. L. (1997) *J. Med. Chem. 40*, 2102−2106.
19. Kuroda, Y., and Kitamura, K. (1984) *J. Am. Chem. Soc.* 106, 1−6.
20. Ellena, J., Dominey, R., Archer, S., Xu, Z., and Cafiso, D. (1987) *Biochemistry 26*, 4584−4592.
21. Wassall, S. R., Ayalasomayajula, S., Griffith, G. L., and McCabe, A. (1993) *Bull. Magn. Reson. 15*, 205−210.
22. Glickson, J. D., Gordon, S. L., Pitner, T. P., Agresti, D. G., and Walter, R. (1976) *Biochemistry 15*, 5721−5729.
23. Henry, G. D., and Sykes, B. D. (1992) *Biochemistry 31*, 5284−5297.
24. Milon, A., Miyazawa, T., and Higashijima, T. (1990) *Biochemistry 29*, 65−75.
25. Jain, M. K., and Wu, N. M. (1977) *J. Membr. Biol. 34*, 157−201.
26. New, R. R. C., Ed. (1990) *Liposomes: A Practical Approach*, pp 45−47, Oxford University Press, London.
27. Qiu, X., and Pidgeon, C. (1993) *Biochemistry 33*, 960−971.
28. Baber, J., Ellena, J. F., and Cafiso, D. S. (1995) *Biochemistry 34*, 6533−6539.
29. Metz, G., Howard, K. P., van Liemt, W. B. S., Prestegard, J. H., Lugtenburg, J., and Smith, S. O. (1995) *J. Am. Chem. Soc. 117*, 564−565.
30. Xiang, T.-X., Anderson, B. D. (1995) *J. Pharm. Sci. 84*, 1308−1315.
31. Pajeva, I. K., Wiese, M., Cordes, H.-P., and Seydel, J. K. (1996) *J. Cancer Res. Clin. Oncol. 122*, 27−40.
32. Zhao, G.-X, Miesbauer, L. R., Smith, D. L., and McLaughlin, J. L. (1994) *J. Med. Chem. 37*, 1971−1976.
33. Neuhaus, D., and Williamson, M. (1989) *The Nuclear Overhauser Effect in Structural and Conformational Analysis*, Chapter 4, VCH Publishers, NewYork.
34. Aksel, A. B., and Noggle, J. H. (1979) *J. Am. Chem. Soc. 101*, 5152−5155.
35. Bloom, M., Evans, E., Mouritsen, O. G. (1991) *Q. Rev. Biophys. 24*, 293−397.
36. Liu, H., Pidgeon, C. (1996) in *Advanced tutorials for the biomedical sciences, animations, simulations, and calculations using mathmatica* (Pidgeon, C., Ed.) pp 19−40, VCH Publishers, New York.
37. Pace, R. J., and Chan, S. I. (1982) *J. Chem. Phys. 76*, 4241−4247.
38. Brown, M. F. (1982) *J. Chem. Phys. 77*, 1576−1599.
39. Gaspar, A. R. M. D., Verschoor, J. A., Neitz, A. W. H., and Vermeulen, N. M. J. (1987) *Biochem. Pharmacol. 36*, 2461−2465.
40. Shiono, Y., and Tsukata, H. (1988) *Jpn. Kokai Tokkyo Koho* JP 63 48,203 [88 48,203].
41. Changonda, L., Lockey, P. M., Marples, B. A., Salt, W. G., and Traynor, J. R. (1989) *Phytother. Res. 3*, 196−200.
42. Qing, Y., Oberlies, N. H., Zeng, L., Shi, G., Evert, D., and McLaughlin, J. L. (1996) *J. Med. Chem. 39*, 1790−1796.
43. Colman-Saizarbitoria, T., Gu, Z.-M., Zhao, G.-X., Zeng, L., Kozlowski, J. F., and McLaughlin, J. L. (1995) *J. Nat. Prod. 58*, 532−539.
44. Naito, H., Kawahara, E., Maruta, K., Maeda, M., and Sasaki, S. (1995) *J. Org. Chem. 60*, 4419−4427.
45. Miyoshi, H., Inoue, M., Okamoto, S., Ohshima, M., Sakamoto, K., and Iwamura, H. (1997) *J. Biol. Chem. 272*, 16176−16183.

BI972348L